



Review

Clinical Usefulness of Right Ventricle–Pulmonary Artery Coupling in Cardiovascular Disease

Qing He^{1,2,3,†}, Yixia Lin^{1,2,3,†}, Ye Zhu^{1,2,3,†}, Lang Gao^{1,2,3}, Mengmeng Ji^{1,2,3}, Li Zhang^{1,2,3,*},
Mingxing Xie^{1,2,3,*} and Yuman Li^{1,2,3,*}

¹ Department of Ultrasound Medicine, Union Hospital, Tongji Medical College, Huazhong University of Science and Technology, Wuhan 430022, China

² Hubei Province Clinical Research Center for Medical Imaging, Wuhan 430022, China

³ Hubei Province Key Laboratory of Molecular Imaging, Wuhan 430022, China

* Correspondence: zli429@hust.edu.cn (L.Z.); xiemx@hust.edu.cn (M.X.); liym@hust.edu.cn (Y.L.);
Tel.: +86-27-85726386 (L.Z. & Y.L.); +86-27-85726430 (M.X.)

† These authors contributed equally to this work.

Abstract: Right ventricular–pulmonary artery coupling (RV-PA coupling) refers to the relationship between RV contractility and RV afterload. Normal RV-PA coupling is maintained only when RV function and pulmonary vascular resistance are appropriately matched. RV-PA uncoupling occurs when RV contractility cannot increase to match RV afterload, resulting in RV dysfunction and right heart failure. RV-PA coupling plays an important role in the pathophysiology and progression of cardiovascular diseases. Therefore, early and accurate evaluation of RV-PA coupling is of great significance for a patient's condition assessment, clinical decision making, risk stratification, and prognosis judgment. RV-PA coupling can be assessed by using invasive or noninvasive approaches. The aim of this review was to summarize the pathological mechanism and evaluation methods of RV-PA coupling, the advantages and disadvantages of each method, and the application value of RV-PA coupling in various cardiovascular diseases.

Keywords: right ventricular–pulmonary artery coupling; pulmonary arterial hypertension; heart failure; valvular heart disease; hypertension



Citation: He, Q.; Lin, Y.; Zhu, Y.; Gao, L.; Ji, M.; Zhang, L.; Xie, M.; Li, Y. Clinical Usefulness of Right Ventricle–Pulmonary Artery Coupling in Cardiovascular Disease. *J. Clin. Med.* **2023**, *12*, 2526. <https://doi.org/10.3390/jcm12072526>

Academic Editors: Antonello D'Andrea and Giovanni La Canna

Received: 28 January 2023

Revised: 2 March 2023

Accepted: 20 March 2023

Published: 27 March 2023



Copyright: © 2023 by the authors. Licensee MDPI, Basel, Switzerland. This article is an open access article distributed under the terms and conditions of the Creative Commons Attribution (CC BY) license (<https://creativecommons.org/licenses/by/4.0/>).

1. Introduction

In recent years, there has been increasing appreciation for the importance of right ventricular (RV) coupling to the pulmonary arterial (PA) circulation, which is called right ventricular–pulmonary artery coupling (RV-PA coupling). RV-PA coupling refers to the relationship between RV contractility and RV afterload and is defined as the ratio of RV end-systolic elastance (contractility index) to PA elastance (arterial load index) [1–5], which is considered to be the gold standard assessment of RV-PA coupling [6–8]. RV function depends on the complex interplay between myocardial contractility and pulmonary vascular afterload [6,9,10]. Normal RV-PA coupling is maintained only when cardiac function and vascular resistance are appropriately matched [11]. At the setting of increased RV afterload, there is preserved RV-PA coupling if RV contractility has increased through RV hypertrophy and adaptation to the load to the level where RV function (cardiac index, tricuspid annular plane systolic excursion (TAPSE), right ventricular ejection fraction (RVEF), etc.) is maintained within a normal range. RV-PA uncoupling occurs when RV contractility cannot increase to match RV afterload, resulting in RV dysfunction and right heart failure [1]. In chronic RV pressure overload, RV-PA uncoupling is considered as the driving cause of RV maladaptation and ultimate RV failure [12]. Therefore, it has important clinical implications for the timely detection of high-risk patients, decision making, and improving the long-term survival of patients. The aim of this review was to summarize pathological mechanism and evaluation methods of RV-PA coupling, the advantages and

disadvantages of each method, and the application value of RV-PA coupling in various cardiovascular diseases.

2. Measurement of Right Ventricular–Pulmonary Artery Coupling

RV-PA coupling is a comprehensive index that requires an overall understanding of RV function and RV afterload, and can be assessed by using integrated hemodynamic parameters related to RV function and afterload [2]. RV-PA coupling is influenced by RV function; however, it is very challenging to achieve a good assessment of RV function [13]. RV-PA coupling can be measured by using invasive and noninvasive ways. The invasive measurement is right heart catheterization (RHC), and noninvasive methods include echocardiography and cardiac magnetic resonance (CMR) imaging. Several measurements for RV-PA coupling are described below. The advantages and disadvantages of each measurement are summarized in Table 1.

Table 1. Advantages and disadvantages of methods evaluating RV-PA coupling.

Index		Advantage	Disadvantage
Invasive	Ees/Ea (gold standard)	High sensitivity and accuracy.	High technical difficulty; Limited bedside application; False normality; Expensive.
	TAPSE/PASP	Easily obtained; Not reliant on image quality; Reproducible.	Angle dependence; Low accuracy in case of TR; Inability to reflect overall RV function.
	RVLS/RVSP	Angle independence; High sensitivity and accuracy; Reproducible; Unaffected by surroundings.	Relies on image quality; Presence of out-of-plane motion of speckles.
Noninvasive	RVFAC/RVSP	Easily obtained; Angle independence; Does not need software analysis.	Depends on image quality.
	RVEF/PASP	Does not rely on the RV geometry assumption.	Low temporal resolution on 3 DE; Depends on image quality.
	SV/ESV	High reliability	May underestimate real RV-PA coupling.
	S' /RVSP	Easily obtained; Independent of image quality; Less dependence on afterload than TAPSE.	Angle dependence. Uses single segment to represent overall RV function.

Ees, end-systolic elastance; Ea, arterial elastance; TAPSE, tricuspid annular plane systolic excursion; PASP, pulmonary arterial systolic pressure; TR, tricuspid regurgitation; RV, right ventricle; RVLS, right ventricular longitudinal strain; RVSP, right ventricular systolic pressure; RVFAC, right ventricular fractional area change; RVEF, right ventricular ejection fraction; 3 DE, three-dimensional echocardiography; SV, stroke volume; ESV, end-systolic volume; RV-PA coupling, right ventricular–pulmonary artery coupling; S', tricuspid annular systolic velocity.

2.1. End-Systolic Elastance/Effective Arterial Elastance

Previous studies have shown that multi-beat end-systolic elastance (Ees)/effective arterial elastance (Ea) from invasive pressure–volume loops by RHC has been regarded as the gold standard for assessment of RV-PA coupling [1,14–18], as other alternative indicators assume a linearity and zero-crossing of end-systolic pressure–volume relationships. Ees is equivalent to cardiac contractility and Ea represents ventricular afterload [19]. Ees is defined as end-systolic pressure (ESP) divided by ventricular end-systolic volume (ESV), which is considered as a load-independent parameter of myocardial contractility [19,20]. Ea is defined as the ratio of ESP divided by the stroke volume (SV) and incorporates all factors of total ventricular afterload, involving peripheral resistance, arterial compliance, and characteristic impedance, and it is a mechanical characteristic that reflects the afterload system functionally [21]. The optimal Ees/Ea ratio is between 1.5 and 2.0, as this can maximize efficiency and minimize energy expenditure [22,23]. This ratio is still preserved

even in the early stages of diseases because of the adaptation to the pressure overload results in concentric RV hypertrophy, which is characterized by an increased wall thickness with almost no change in the chamber volume; thus, RV Ees matches the elevated Ea. Only with progressive RV decompensation does RV Ees begin to fall with an inability to match an increase in Ea; Ees/Ea declines, the mechanical work efficiency will be low, and lastly, RV-PA coupling becomes uncoupled [20]. The methods for measuring Ees/Ea include single-beat and multiple-beat. At present, multiple-beat methods are more valuable in practice. Uncertainties in maximum pressure (Pmax) calculations and the imperfect linearity of end-systolic pressure–volume relationships may result in disagreement between single-beat and multiple-beat methods [24]. The advantages of Ees/Ea in assessing RV-PA coupling are its high sensitivity and accuracy [6,25]. However, it also has various defects, which include that it is invasive and technically demanding, expensive, and unpractical at the bedside [15]. Moreover, both Ees and Ea may become abnormal with disease progression, but the Ees/Ea ratio may be close to normal instead. To surmount the above limitations, more and more researchers have explored other accessible, convenient, noninvasive alternatives to measuring RV-PA coupling.

2.2. Noninvasive Methods

2.2.1. Tricuspid Annular Plane Systolic Excursion/Pulmonary Arterial Systolic Pressure

TAPSE is the most frequently used echocardiographic parameter of RV systolic function in clinical settings (Figure 1A). Pulmonary arterial systolic pressure (PASP), as a Doppler index of RV afterload, is also easily acquired by echocardiography. TAPSE/PASP, as a method for the noninvasive measurement of RV-PA coupling, has gradually become an alternative parameter for Ees/Ea [26–32]. It was shown that TAPSE/PASP was strongly correlated with the invasive assessment of RV-PA coupling [15]. A decreased TAPSE/PASP ratio suggests the decoupling of RV contractility from its afterload [21,33–35]; the cut-off value for abnormally low TAPSE/PASP was 0.36 mm/mmHg, below which RV-PA coupling was considered compromised. TAPSE is easy to obtain, being independent of image quality and highly reproducible [36]. However, TAPSE is limited by angle dependence and less accuracy in the case of severe tricuspid regurgitation (TR) [37]. In addition, TAPSE represents only the longitudinal movement of the basal segment of the RV free wall and may fail to accurately reflect the entire RV function, especially in patients with RV regional wall motion abnormalities. Increasing numbers of studies have applied TAPSE/PASP to assess the balance between RV function and pulmonary circulation, and it has become a simple, noninvasive, and effective surrogate of Ees/Ea.

2.2.2. Tricuspid Annular Systolic Velocity/Right Ventricular Systolic Pressure

Tricuspid annular systolic velocity (S') measured by tissue Doppler imaging is another highly reproducible indicator of longitudinal RV contractility of the basal RV free wall (Figure 1B). S' /right ventricular systolic pressure (RVSP) integrates both RV systolic function and RV afterload, and therefore, it can be used to evaluate RV-PA coupling. A reduced S' /RVSP has been reported as a vital prognostic marker associated with high mortality in cardiac intensive care patients and could be used for risk stratification of critically ill patients; in addition, S' /RVSP highly correlates with TAPSE/PASP [38]. S' is easily obtained and not affected by image quality, and it depends less on the afterload than TAPSE. Yet, it is angle-dependent. In addition, it assumes that the function of a single RV segment represents the entire RV function, which is less accurate in RV infarction or pulmonary embolism. RVFAC, S' , and TAPSE using two-dimensional echocardiography are shown in Figure 1.

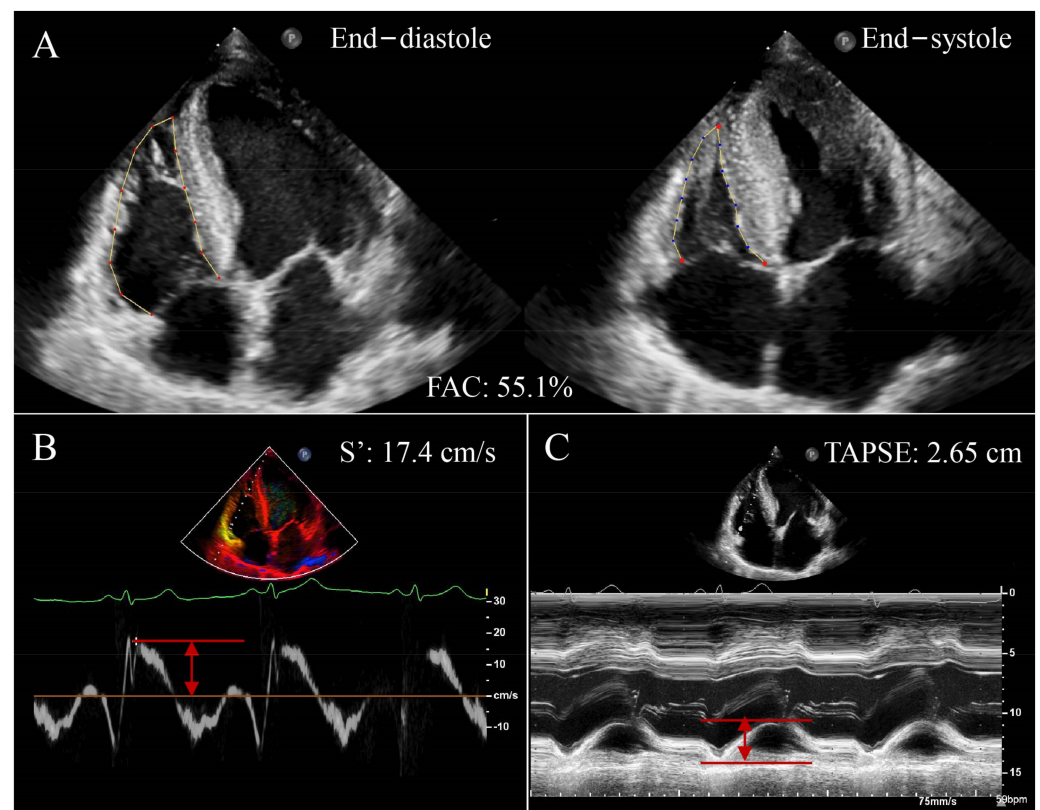


Figure 1. Conventional RV function parameters using two-dimensional echocardiography in a patient with HFrEF. (A) RVFAC; (B) S' ; (C) TAPSE; RV, right ventricular; HFrEF, heart failure with reduced ejection fraction; RVFAC, right ventricular fractional area change; S' , tricuspid annular systolic velocity; TAPSE, tricuspid annular plane systolic excursion. Red arrows represent measurements for parameters.

2.2.3. Right Ventricular Fractional Area Change/Right Ventricular Systolic Pressure

Right ventricular fractional area change (RVFAC) reflects RV longitudinal and transverse systolic function and is calculated as $(RV \text{ end-diastolic area} - RV \text{ end-systolic area}) / RV \text{ end-diastolic area} \times 100\%$ (Figure 1C) [39]. The ratio of RVFAC/RVSP can be used as a noninvasive method to assess RV-PA coupling. The RVFAC/RVSP ratio has been confirmed to be of superior prognostic value compared with RV systolic function (TAPSE or RVFAC) alone [40]. RVFAC is highly correlated with RVEF and has been reported as a simple and rapid method to evaluate RV systolic function. The RVFAC/RVSP ratio is easy to acquire, angle-independent, and does not require additional analysis software [41]. Nevertheless, RVFAC measurement requires the delineation of RV endocardial borders, and RVFAC accuracy may be compromised when image quality is poor.

2.2.4. Stroke Volume/End-Systolic Volume

As mentioned earlier, E_{es} is calculated as ESP/ESV and E_a is calculated as ESP/SV . Both have a common ESP, so the RV-PA coupling ratio can be further simplified as SV/ESV , which is an alternative volume-based method to RV-PA coupling assessment [42,43]. In a study cohort of pediatric pulmonary arterial hypertension (PAH), which indicated the feasibility of the SV/ESV ratio derived from CMR, it was found that it correlated with the RV-PA coupling ratio evaluated by cardiac catheterization [44]. SV/ESV has been demonstrated to have application value in dilated cardiomyopathy (DCM), PAH, and other diseases [42,44–46]. The SV/ESV ratio can also be derived from three-dimensional echocardiography (3 DE). The 3 DE determined SV/ESV ratio has been shown to have a strong correlation with right-heart-catheterization-derived RV-PA coupling in adults with PAH [46]. The limitation of the SV/ESV ratio is that it is a simplified E_{es}/E_a and may

underestimate E_{es}/E_a in practice [47,48]. Compared with E_{es}/E_a , SV/ESV assumes the linearity and zero-crossing of end-systolic pressure–volume relationships, which may result in moderately increased bias [24].

2.2.5. Right Ventricular Longitudinal Strain/Right Ventricular Systolic Pressure

Recently, right ventricular longitudinal strain (RVLS) obtained by two-dimensional speckle tracking echocardiography has been demonstrated to be a more sensitive indicator for RV function than conventional echocardiographic parameters, and it can detect sub-clinical myocardial dysfunction earlier [49]. The assessment of right ventricular global longitudinal strain is displayed in Figure 2. Therefore, the ratio of RVLS to PASP corresponds to the ratio of RV systolic function to RV afterload, and has been proposed to correlate with the E_{es}/E_a ratio [50–52]. RVLS is noninvasive and angle-independent, has excellent accuracy and reproducibility, and is not affected by surrounding tissue structure and respiratory movement. However, two-dimensional speckle tracking echocardiography is hampered by image quality, 2D plane measurement, and the out-of-plane motion of speckles [53].

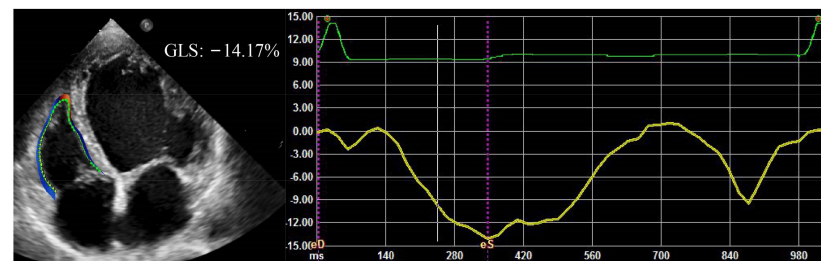


Figure 2. RVGLS in a patient with HF rEF. RVGLS, right ventricular global longitudinal strain.

2.2.6. Right Ventricular Ejection Fraction/Pulmonary Arterial Systolic Pressure

RVEF is the most common used index of RV systolic function in everyday clinical practice and is strongly predictive of adverse outcomes in patients with a variety of cardiovascular diseases [54,55]. It has been confirmed that a lower RVEF/PASP ratio was associated with an increased risk of heart failure (HF) or death [37]. RVEF can be measured by 3 DE and CMR, and it does not rely on the RV geometry assumption. The analysis of RVEF using 3 DE is shown in Figure 3. However, 3 DE is hindered by a lower temporal resolution and is dependent on the image quality [56].

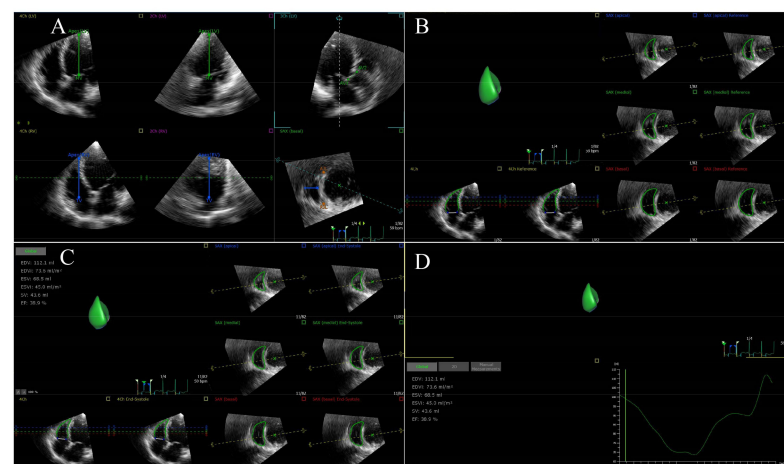


Figure 3. RVEF using 3 DE in a patient with HF rEF. (A) Setting reference points; (B) RV endocardial border identification and tracking at end-diastole; (C) RV endocardial border identification and tracking at end-systole; (D) RVEF is automatically generated. RVEF, right ventricular ejection fraction; 3 DE, three-dimensional echocardiography.

3. Clinical Applications of RV-PA Coupling

3.1. Pulmonary Arterial Hypertension

The level of clinical treatment continues to improve, but the quality of life and prognosis of PAH patients are still unsatisfying [56,57]. PAH leads to RV pressure overload due to increased PVR and is unable to maintain normal RV cardiac output; thereby, it results in the decoupling of RV-PA and ultimate RV failure and death [58–61]. RV-PA coupling is crucial for the risk stratification of PAH patients [2,62,63]. In a study involving 26 patients with PAH, they underwent CMR, RHC, and RV pressure–volume assessment with multi-beat (MB) determination of Ees/Ea on the same day, and follow-up to observe their disease development [6]. The investigators found 16 subjects eventually met the criteria for clinical worsening, and they were more likely to have a lower MB Ees/Ea ratio (0.7 ± 0.5 versus 1.3 ± 0.8 , $p = 0.02$), and MB Ees/Ea predicted the time to clinical worsening in PAH. In addition, MB Ees/Ea was shown to be superior to RVEF and SV/ESV in its ability to predict CW in human PAH [6]. RV-PA coupling was relatively maintained in earlier stages but was impaired markedly with more severe PAH in 139 adults with PAH [42]. In the above study, contractility was augmented to match the increased load and maintained the SV in the early phases of chronic PAH, preserving optimal coupling at the expense of suboptimal mechanical efficiency. Ultimately, RV failed as a pump, which indicated inadequate coupling and reduced myocardial efficiency. This study demonstrated that the evaluation of RV-PA coupling may help to expound the mechanisms of RV failure and to identify patients at risk, or guide the timing of therapeutic interventions in PAH [42]. In a study of 203 patients with PAH, RV volume, RVEF, RVLS, and the RVEF/PASP ratio were measured using 3D echocardiography [37]. Their findings showed that RV-PA coupling declined with the advancing World Health Organization functional class (WHO-FC). Patients with WHO-FC I and II had a significantly higher RVEF/PASP ratio than patients with WHO-FC III and IV (both $p < 0.001$). Additionally, PAH is one of the most important factors for the evaluation of patients before heart transplant, which is associated with prognosis after heart transplant [64]. In a study cohort of 44 heart transplant recipients, it was shown that RV-PA coupling is impaired early after heart transplant and improves significantly from 7 to 30 days post-transplant, and the evolution is correlated with donor–recipient size matching. The interaction between RV-PA coupling and donor–recipient size matching may play an important role in preventing major RV dysfunction in patients post-heart transplant [65]. Thus, the evaluation of RV-PA coupling is beneficial for the early identification of high-risk patients with PAH and the clinical management of patients as well as the prediction of outcomes.

3.2. Heart Failure

HF is a clinical syndrome in which symptoms and/or signs are caused by structural and/or functional abnormalities of the heart, as evidenced by elevated levels of brain natriuretic peptide and/or objective evidence of pulmonary or systemic congestion [66–70]. HF can be divided into three types: heart failure with preserved ejection fraction (HFpEF), heart failure with mid-range ejection fraction (HfmrEF), and heart failure with reduced ejection fraction (HfrEF) [66,70–72]. Considerable evidence has demonstrated that assessment of RV-PA coupling plays a crucial role in risk stratification, monitoring efficacy, and predicting outcomes in HF patients [14,31,73]. Since there are few studies on HfmrEF at present, the application of RV-PA coupling in HF mainly focuses on the following two aspects.

3.2.1. Heart Failure with Preserved Ejection Fraction

HfpEF accounts for about half of HF patients [74], and it was previously thought to be mainly a disorder of left ventricular (LV) diastolic function [75–82]. Previous researches have revealed that both pulmonary circulation and RV function are impaired in HfpEF patients [83–88]. In a study cohort of 67 patients with HfpEF, which applied Ees/Ea to evaluate RV-PA coupling in HfpEF patients at rest and during exercise, the results showed that RV-PA coupling was significantly lower in HfpEF patients at rest compared with the

controls [89]. Ees/Ea was elevated in HfpEF patients during the initial stage of exercise, which may be associated with a significant increase in RV contractility, but RV-PA coupling worsened during peak exercise. Evidence shows that RV-PA coupling is a favorable indicator of exercise tolerance in HfpEF patients and can assist in guiding treatment to improve exercise tolerance [89]. A study including 384 patients with HfpEF indicated that TAPSE was associated closely with PASP in HfpEF patients, and combining the information on RV function and pulmonary artery pressures in a single TAPSE/PASP ratio allowed us to obtain an accurate risk stratification in all HF patients [33]. Further research that involved 387 patients with HfpEF compared RV contractile function and RV-PA coupling in HfpEF patients with variable disease severity stratified according to TAPSE/PASP ratio tertile (1: <0.35 ; 2: 0.35 to 0.57 ; 3: >0.57) [26]. They found that patients in tertile 1 presented with higher PASP and RV end-diastolic and end-systolic areas, and lower TAPSE and RVFAC. Their results demonstrated that the TAPSE/PASP ratio was inversely correlated with the New York Heart Association functional class and could independently predict adverse outcomes. Therefore, the TAPSE/PASP ratio seems helpful in unmasking the early occurrence of symptoms and an initial depression in the RV functional reserve [26]. In a prospective research study, HfpEF patients had a decreased RV systolic reserve and abnormal RV-PA coupling in the early stage of disease, but the aforementioned parameters were largely reversible [90]. RV-PA coupling was enhanced with β -adrenergic stimulation in HfpEF subjects, which confirmed that interventions targeting RV function or afterload may be beneficial for patients at an early stage of disease progression [90]. Additionally, investigators studied the occurrence of pulmonary interstitial edema in patients with HfpEF, and assessed RV-PA coupling using three indicators: TAPSE/PASP, $S'/PASP$, and RVFAC/RVSP [91]. The above study revealed that three indicators were reduced in patients with HfpEF compared with the healthy controls. These findings demonstrated that pulmonary interstitial edema may be associated with abnormal RV-PA coupling, and early measurement of RV-PA coupling could predict the occurrence of pulmonary interstitial edema in HfpEF patients [91]. In conclusion, the evaluation of RV-PA coupling may be crucial to identify patients at higher risk, delay disease progression, and improve the prognosis for patients with HfpEF.

3.2.2. Heart Failure with Mid-Range Ejection Fraction

The pathological process of HfrEF is similar to HfpEF, but it has a high incidence as well as poor prognosis. HfrEF is often accompanied by PAH, which can significantly affect disease progression and prognosis; thus, it is crucial to evaluate RV-PA coupling in patients with HfrEF. In a study cohort of 112 patients with HfrEF, Ees/Ea was closely associated with RV function and predicted the overall survival of HfrEF patients [92]. Furthermore, the best cut-off for Ees/Ea to discriminate overall survival was 0.68, and patients with Ees/Ea <0.68 were characterized by significantly lower intrinsic RV contractility and higher afterload parameters (Ea or PVR) than those with Ees/Ea ≥ 0.68 . Hence, Ees/Ea evaluation was beneficial for a better clinical risk stratification and decision-making process for the timing of LV assist devices and/or heart transplantation in patients with HfrEF [92]. In a study including 205 HfrEF patients who underwent an overall assessment with echocardiography and exercise tolerance tests, a lower TAPSE/PASP was correlated with lower functional class, exercise capacity, and ventilatory inefficiency, and was predictive of adverse outcomes among patients with HfrEF [93]. Hence, the TAPSE/PASP ratio would be a helpful screening marker to identify patients with HfrEF with severely impaired exercise tolerance and triage them to a specific cardiopulmonary exercise test as needed [93]. In a cohort of 54 patients with HfrEF undergoing cardiac resynchronization therapy, it was demonstrated that TAPSE/PASP displayed good sensitivity (90%) and specificity (81.8%) for predicting the response to cardiac resynchronization therapy. Moreover, a lower TAPSE/PASP ratio was associated with a higher incidence of adverse cardiovascular events during the follow-up [94]. Hence, these findings suggested that the TAPSE/PASP ratio may become a

standard echocardiographic evaluation parameter for HfrEF patients undergoing cardiac resynchronization therapy.

3.3. Hypertension

Compared to the left heart, a few studies have investigated RV function in hypertensive patients. Actually, long-term overload of the left ventricle can result in increased pressure and injury, with intimal fibrosis and remodeling on the pulmonary vessels, leading to elevated PVR, PA pressure, and RV afterload, and ultimately right ventricular dysfunction came up [95]. Patients with uncontrolled and untreated hypertension have worse RV and atrial mechanics, as well as functional capacity, in comparison with the better treated hypertensive patients [96]. In a study of 446 hypertensive patients with different glucose tolerance levels, patients were graded as the normal glucose tolerance 1 group with 1 h post-load plasma glucose < 155 mg/dL, the NGT 2 group with 1 h post-load plasma glucose \geq 155 mg/dL, the impaired glucose tolerance group, and the type 2 diabetes mellitus group, from low to high according to 1 h post-load plasma glucose. In this study, the value of PASP and PVR were significantly higher from the first to the fourth group, as well as a reduction in RV function parameters demonstrated by lower TAPSE/PASP, TAPSE, and RVFAC. Not only the left heart but also the RV was affected by early glucose metabolism disorders. Monitoring RV-PA coupling in hypertensive patients could provide timely identification of right heart injury caused by impaired glucose tolerance, and improve long-term survival [97]. Furthermore, RV-PA coupling assessed by TAPSE/PASP was compared between the control group and the hypertensive group [98]. They found that TAPSE/PASP in the hypertensive group was significantly lower than that in control group [98]. Thus, accurate assessment of RV-PA coupling could be helpful to reduce the mortality, assist patients with treatment, and decrease the incidence of cardiovascular-related events.

3.4. Valvular Heart Disease

The tricuspid valve is closely related to RV and PA. A study investigating 1149 patients with secondary TR applied TAPSE/PASP to estimate whether RV-PA coupling could improve risk stratification and showed that 470 patients had a decreased TAPSE/PASP ratio; that is, decoupling of RV-PA, and patients with decoupled RV-PA had a higher incidence of symptoms and comorbidities, with more severe TR and RV remodeling [99]. In addition, in a series of 444 TR patients undergoing transcatheter tricuspid valve repair or replacement (TTVR), multivariable Cox regression analysis showed that a higher TAPSE/PASP ratio was associated with a declined risk of all-cause mortality, and the magnitude of TR reduction after TTVR was independently related with a reduction in post-TTVR RV-PA coupling. These results revealed that RV-PA coupling may be helpful to patient selection and prognostication following TTVR [100]. A study that involved 372 patients with HF and severe secondary mitral regurgitation reported that patients with a lower RVLS/RVSP ratio had larger mean proximal isovelocity surface area-derived effective regurgitant orifice areas and were more likely to have severe (4+) mitral regurgitation [50]. By multivariable analysis, impaired RV-PA coupling was strongly associated with enhanced risk for death or hospitalization in patients with HF and secondary mitral regurgitation. Patients with RV-PA uncoupling experienced more New York Heart Association functional class III or IV symptoms compared with those with normal RV-PA coupling [50]. A study evaluated S' /RVSP by echocardiography to investigate RV-PA coupling in patients with aortic stenosis who experienced transcatheter aortic valve replacement, and they found that S' was increased in aortic stenosis patients after transcatheter aortic valve replacement, indicating enhanced RV-PA coupling [101]. This study demonstrated that S' /RVSP could monitor the changes in condition of patients with aortic stenosis, clarify the efficacy of transcatheter aortic valve replacement, and facilitate the timely adjustment of treatment [101]. Thus, RV-PA coupling plays a key role in risk stratification, the prediction of clinical outcomes, and in guiding treatment in patients with valvular heart disease.

3.5. Congenital Heart Disease

Tetralogy of Fallot (TOF) is the most frequent cyanotic congenital heart disease. Patients with repaired TOF commonly develop RV dilatation, which can cause progressive RV failure. Previous studies primarily focused on the evaluation of RV dimensions and function, but RV is coupled to the low-pressure PA system with high compliance [21]. Therefore, the RV and pulmonary artery should be assessed as a whole in patients with repaired TOF. In a retrospective study of 129 adults (repaired TOF ($n = 84$) and VPS with previous intervention ($n = 45$)), RV-PA coupling was lower in the TOF group FAC/RVSP (ratio 1.10 ± 0.29 vs. 1.48 ± 0.22 ($p < 0.001$)) and TAPSE/RVSP ratio (0.51 ± 0.15 vs. 0.78 ± 0.11 ($p < 0.001$)) compared to the healthy controls because of a higher RV afterload (RVSP 42 ± 3 mm Hg vs. 31 ± 3 mmHg ($p = 0.012$)) [40]. Similar results were seen in the VPS group. A reduction in RV-PA coupling caused by a disproportionate increase in PA elastance highlighted the important role of abnormal PA elastic properties and its potential interaction with RV-PA coupling in TOF and VPS patients with PR [40]. Additionally, investigators aimed to determine the association between noninvasive RV-PA coupling indices (TAPSE/RVSP and FAC/RVSP ratio) and disease severity in TOF patients, and compared this association to peak oxygen consumption [102]. They found that RV-PA coupling was modestly correlated with peak oxygen consumption in patients with TOF. Their findings highlighted the importance of noninvasive RV-PA coupling indices as a potential supplementary tool in the evaluation of patients with TOF [102]. By evaluating RV-PA coupling, a study including 24 patients provided new insights in searching for additional mechanisms for the deterioration in RV performance and the response to therapeutic interventions in the long-term follow-up of patients with repaired TOF [21]. This study elucidated the emerging role of RV-PA coupling as a contributing mechanism for the decline in RV function and impaired effect to inotropic drugs in patients with TOF [21]. In a retrospective study of 135 patients with post-operative TOF, the data showed that RV-PA uncoupling was prevalent in repaired TOF patients, and the uncoupling group had obvious lower TAPSE/PASP compared with the coupling group [19]. Furthermore, their results indicated that the TAPSE/PASP ratio came out as the strongest predictor for RV-PA uncoupling, helping to provide additional understanding of the decline in RV performance [19]. Thus, RV-PA coupling exerts a major influence on risk stratification and outcome prediction in patients after TOF.

3.6. Cardiomyopathy

DCM is characterized by the presence of systolic dysfunction and LV or biventricular dilatation and in the absence of coronary artery disease or abnormal loading conditions, which frequently has a genetic background [103]. Recently, the long-term survival of DCM patients has increased significantly. It remains the most common reason for heart transplant in the Western world nevertheless [104]. Originally, the RV adapts by remodeling and hypertrophy, leading to an initial increase in contractility. RV maladaptation occurs with disease progression, and the RV begins to dilate, followed by the decoupling of RV-PA [65]. Another study investigated the RV-PA coupling defined as the SV/ESV ratio in 139 outpatients with DCM, and reported that RV-PA coupling was significantly more impaired with increasing symptom severity, and was the only independent determinant of severe DCM, regardless of age, diuretic use, LV systolic function, LV diastolic function, and PASP [45]. Therefore, RV-PA coupling was further proposed as a marker of disease severity in DCM patients. One of the earliest studies to assess RV-PA coupling as an outcome predictor in DCM, which included 60 patients with DCM who were followed for a mean period of 18 months, revealed that noninvasive RV-PA coupling was more significantly impaired in patients with DCM who were rehospitalized for HF exacerbation, and the RVLS/PASP ratio and the RVEF/PASP ratio were independent predictors of rehospitalizations. The cut-off values for RVLS/PASP and RVEF/PASP were -0.40 and -1.30 , respectively [105]. Hirasawa et al. demonstrated that a low TAPSE/SPAP ratio was

associated with adverse outcomes in hypertrophic cardiomyopathy (HCM), and RV-PA coupling could be important in risk stratification of patients with HCM [106].

4. Summary and Prospect

Decoupling of RV-PA is the terminal state of various cardiovascular diseases and poses a great harm to the health of patients. Therefore, early and accurate evaluation of RV-PA coupling in patients has important clinical value for the early identification of high-risk patients, delaying disease progression, guiding treatment, and improving prognosis. At present, various methods for RV-PA coupling assessment have been employed, including invasive and noninvasive approaches. The gold standard measurement of RV-PA coupling is Ees/Ea obtained by RHC, which is invasive, complex, and not widely available. It is expected to replace invasive techniques as the preferred method in the future with the continuous development of easy and noninvasive techniques such as Large sample, and prospective studies are needed to clarify the optimal application parameters of the noninvasive estimation of RV-PA coupling in order to help doctors to provide better management of patients.

Author Contributions: Conceptualization, Q.H. and Y.Z.; methodology, Q.H., L.G., L.Z., M.X. and Y.L. (Yuman Li); software, Q.H., Y.Z., Y.L. (Yixia Lin) and M.J.; writing—original draft preparation, Q.H., Y.Z., Y.L. (Yixia Lin), L.G., M.J., L.Z., M.X. and Y.L. (Yuman Li); writing—review and editing, Q.H., Y.L. (Yixia Lin), L.G. and M.J.; funding acquisition, L.Z., M.X. and Y.L. (Yuman Li). All authors have read and agreed to the published version of the manuscript.

Funding: This research was funded by the National Natural Science Foundation of China (Grant Nos. 82230066, 82151316, 82171964), the Key Research and Development Program of Hubei (Grant Nos. 2020DCD015, 2021BCA138), and the Hubei Natural Science Funds for Distinguished Young Scholars (2021CFA046).

Institutional Review Board Statement: Not applicable.

Informed Consent Statement: Not applicable.

Data Availability Statement: Not applicable.

Conflicts of Interest: The authors declare no conflict of interest.

References

1. Jone, P.N.; Ivy, D.D. Comprehensive Noninvasive Evaluation of Right Ventricle-Pulmonary Circulation Axis in Pediatric Patients with Pulmonary Hypertension. *Curr. Treat. Options Cardiovasc. Med.* **2019**, *21*, 6. [\[CrossRef\]](#)
2. Kubba, S.; Davila, C.D.; Forfia, P.R. Methods for Evaluating Right Ventricular Function and Ventricular-Arterial Coupling. *Prog. Cardiovasc. Dis.* **2016**, *59*, 42–51. [\[CrossRef\]](#)
3. Monge García, M.I.; Santos, A. Understanding ventriculo-arterial coupling. *Ann. Transl. Med.* **2020**, *8*, 795. [\[CrossRef\]](#)
4. Naeije, R.; Brimiouille, S.; Dewachter, L. Biomechanics of the right ventricle in health and disease (2013 grover conference series). *Pulm. Circ.* **2014**, *4*, 395–406. [\[CrossRef\]](#)
5. Amsallem, M.; Mercier, O.; Kobayashi, Y.; Moneghetti, K.; Haddad, F. Forgotten No More: A Focused Update on the Right Ventricle in Cardiovascular Disease. *JACC Heart Fail.* **2018**, *6*, 891–903. [\[CrossRef\]](#)
6. Hsu, S.; Simpson, C.E.; Houston, B.A.; Wand, A.; Sato, T.; Kolb, T.M.; Mathai, S.C.; Kass, D.A.; Hassoun, P.M.; Damico, R.L.; et al. Multi-beat right ventricular-arterial coupling predicts clinical worsening in pulmonary arterial hypertension. *J. Am. Heart Assoc.* **2020**, *9*, e016031. [\[CrossRef\]](#)
7. Inuzuka, R.; Hsu, S.; Tedford, R.J.; Senzaki, H. Single-beat estimation of right ventricular contractility and its coupling to pulmonary arterial load in patients with pulmonary hypertension. *J. Am. Heart Assoc.* **2018**, *7*, e007929. [\[CrossRef\]](#)
8. Richter, M.J.; Hsu, S.; Yogeswaran, A.; Husain-Syed, F.; Vadász, I.; Ghofrani, H.A.; Naeije, R.; Harth, S.; Grimminger, F.; Seeger, W.; et al. Right ventricular pressure-volume loop shape and systolic pressure change in pulmonary hypertension. *Am. J. Physiol. Lung Cell. Mol. Physiol.* **2021**, *320*, L715–L725. [\[CrossRef\]](#)
9. Newman, J.H.; Brittain, E.L.; Robbins, I.M.; Hemnes, A.R. Effect of acute arteriolar vasodilation on capacitance and resistance in pulmonary arterial hypertension. *Chest* **2015**, *147*, 1080–1085. [\[CrossRef\]](#)
10. Noordegraaf, A.V.; Chin, K.M.; Haddad, F.; Hassoun, P.M.; Hemnes, A.R.; Hopkins, S.R.; Kawut, S.M.; Langleben, D.; Lumens, J.; Naeije, R.; et al. Pathophysiology of the right ventricle and of the pulmonary circulation in pulmonary hypertension: An update. *Eur. Respir. J.* **2019**, *53*, 1801900. [\[CrossRef\]](#)

11. Deng, Y.; Guo, S.L. Research progress of stress ultrasonography and its evaluation of right ventricular-pulmonary artery coupling. *Guangxi Med.* **2019**, *41*, 617–623.
12. Antonini-Canterin, F.; Di Nora, C. Arrhythmogenic right ventricular cardiomyopathy or athlete's heart? Challenges in assessment of right heart morphology and function. *Monaldi Arch. Chest Dis.* **2019**, *89*, 1047. [[CrossRef](#)]
13. Tello, K.; Dalmer, A.; Vanderpool, R.; Ghofrani, H.A.; Naeije, R.; Roller, F.; Seeger, W.; Wilhelm, J.; Gall, H.; Richter, M.J. Cardiac Magnetic Resonance Imaging-Based Right Ventricular Strain Analysis for Assessment of Coupling and Diastolic Function in Pulmonary Hypertension. *JACC Cardiovasc. Imaging* **2019**, *12*, 2155–2164. [[CrossRef](#)]
14. Ikonomidis, I.; Aboyans, V.; Blacher, J.; Brodmann, M.; Brutsaert, D.L.; Chirinos, J.A.; De Carlo, M.; Delgado, V.; Lancellotti, P.; Lekakis, J.; et al. The role of ventricular–arterial coupling in cardiac disease and heart failure: Assessment, clinical implications and therapeutic interventions. A consensus document of the European Society of Cardiology Working Group on Aorta & Peripheral Vascular Diseases. *Eur. J. Heart Fail.* **2019**, *21*, 402–424. [[CrossRef](#)]
15. Tello, K.; Wan, J.; Dalmer, A.; Vanderpool, R.; Ghofrani, H.A.; Naeije, R.; Roller, F.; Mohajerani, E.; Seeger, W.; Herberg, U.; et al. Validation of the Tricuspid Annular Plane Systolic Excursion/Systolic Pulmonary Artery Pressure Ratio for the Assessment of Right Ventricular-Arterial Coupling in Severe Pulmonary Hypertension. *Circ. Cardiovasc. Imaging* **2019**, *12*, e009047. [[CrossRef](#)]
16. Schmeisser, A.; Rauwolf, T.; Groscheck, T.; Kropf, S.; Luani, B.; Tanev, I.; Hansen, M.; Meißler, S.; Steendijk, P.; Braun-Dullaues, R.C.; et al. Pressure-volume loop validation of TAPSE/PASP for right ventricular arterial coupling in heart failure with pulmonary hypertension. *Eur. Heart J. Cardiovasc. Imaging* **2021**, *22*, 168–176. [[CrossRef](#)]
17. Nguyen, M.; Berhoud, V.; Bartamian, L.; Martin, A.; Ellouze, O.; Bouhemad, B.; Guinot, P.G. Agreement between different non-invasive methods of ventricular elastance assessment for the monitoring of ventricular-arterial coupling in intensive care. *J. Clin. Monit. Comput.* **2020**, *34*, 893–901. [[CrossRef](#)]
18. Sanz, J.; Sánchez-Quintana, D.; Bossone, E.; Bogaard, H.J.; Naeije, R. Anatomy, Function, and Dysfunction of the Right Ventricle: JACC State-of-the-Art Review. *J. Am. Coll. Cardiol.* **2019**, *73*, 1463–1482. [[CrossRef](#)]
19. Sandeep, B.; Cheng, H.; Luo, L.; Li, Y.; Xiong, D.; Gao, K.; Xiao, Z. Assessing Right Ventricle Pulmonary Artery Coupling and Uncoupling Using Echocardiography and Cardiopulmonary Exercise Test in Post Operative TOF Patients. *Curr. Probl. Cardiol.* **2022**, 101214. [[CrossRef](#)]
20. Sunagawa, K.; Maughan, W.L.; Burkhoff, D.; Sagawa, K. Coupling Right Ventricular–Pulmonary Arterial Research to the Pulmonary Hypertension Patient Bedside. *Am. J. Physiol. Heart Circ. Physiol.* **1983**, *14*, e005715. [[CrossRef](#)]
21. Latus, H.; Binder, W.; Kerst, G.; Hofbeck, M.; Sieverding, L.; Apitz, C. Right ventricular-pulmonary arterial coupling in patients after repair of tetralogy of Fallot. *J. Thorac. Cardiovasc. Surg.* **2013**, *146*, 1366–1372. [[CrossRef](#)]
22. Vonk-Noordegraaf, A.; Haddad, F.; Chin, K.M.; Forfia, P.R.; Kawut, S.M.; Lumens, J.; Naeije, R.; Newman, J.; Oudiz, R.J.; Provencher, S.; et al. Right heart adaptation to pulmonary arterial hypertension: Physiology and pathobiology. *J. Am. Coll. Cardiol.* **2013**, *62* (Suppl. S25), 22–33. [[CrossRef](#)]
23. Lahm, T.; Douglas, I.S.; Archer, S.L.; Bogaard, H.J.; Chesler, N.C.; Haddad, F.; Hemnes, A.R.; Kawut, S.M.; Kline, J.A.; Kolb, T.M.; et al. Assessment of right ventricular function in the research setting: Knowledge gaps and pathways forward an official American thoracic society research statement. *Am. J. Respir. Crit. Care Med.* **2018**, *198*, e15–e43. [[CrossRef](#)]
24. Richter, M.J.; Peters, D.; Ghofrani, H.A.; Naeije, R.; Roller, F.; Sommer, N.; Gall, H.; Grimminger, F.; Seeger, W.; Tello, K. Evaluation and prognostic relevance of right ventricular-arterial coupling in pulmonary hypertension. *Am. J. Respir. Crit. Care Med.* **2020**, *201*, 116–119. [[CrossRef](#)]
25. Hsu, S.; Houston, B.A.; Tampakakis, E.; Bacher, A.C.; Rhodes, P.S.; Mathai, S.C.; Damico, R.L.; Kolb, T.M.; Hummers, L.K.; Shah, A.A.; et al. Right ventricular functional reserve in pulmonary arterial hypertension. *Circulation* **2016**, *133*, 2413–2422. [[CrossRef](#)]
26. Guazzi, M.; Dixon, D.; Labate, V.; Beussink-Nelson, L.; Bandera, F.; Cuttica, M.J.; Shah, S.J. RV Contractile Function and its Coupling to Pulmonary Circulation in Heart Failure with Preserved Ejection Fraction Stratification of Clinical Phenotypes and Outcomes. *JACC Cardiovasc. Imaging* **2017**, *10*, 1211–1221. [[CrossRef](#)]
27. Marra, A.M.; Sherman, A.E.; Salzano, A.; Guazzi, M.; Saggari, R.; Squire, I.B.; Cittadini, A.; Channick, R.N.; Bossone, E. Right Side of the Heart Pulmonary Circulation Unit Involvement in Left-Sided Heart Failure: Diagnostic, Prognostic, and Therapeutic Implications. *Chest* **2022**, *161*, 535–551. [[CrossRef](#)]
28. Santas, E.; Palau, P.; Guazzi, M.; De La Espriella, R.; Miñana, G.; Sanchis, J.; Bayes-Genís, A.; Lupón, J.; Chorro, F.J.; Núñez, J. Usefulness of Right Ventricular to Pulmonary Circulation Coupling as an Indicator of Risk for Recurrent Admissions in Heart Failure with Preserved Ejection Fraction. *Am. J. Cardiol.* **2019**, *124*, 567–572. [[CrossRef](#)]
29. Bragança, B.; Trêpa, M.; Santos, R.; Silveira, I.; Fontes-Oliveira, M.; Sousa, M.J.; Reis, H.; Torres, S.; Santos, M. Echocardiographic assessment of right ventriculo-arterial coupling: Clinical correlates and prognostic impact in heart failure patients undergoing cardiac resynchronization therapy. *J. Cardiovasc. Imaging* **2020**, *28*, 109–120. [[CrossRef](#)]
30. Rosa, G.M.; D'Agostino, A.; Giovinazzo, S.; La Malfa, G.; Fontanive, P.; Miccoli, M.; Dini, F.L. Echocardiography of right ventricular-arterial coupling predicts survival of elderly patients with heart failure and reduced to mid-range ejection fraction. *Monaldi Arch. Chest Dis.* **2020**, *90*. [[CrossRef](#)] [[PubMed](#)]
31. Ghio, S.; Gavazzi, A.; Campana, C.; Inserra, C.; Klersy, C.; Sebastiani, R.; Arbustini, E.; Recusani, F.; Tavazzi, L. Independent and additive prognostic value of right ventricular systolic function and pulmonary artery pressure in patients with chronic heart failure. *J. Am. Coll. Cardiol.* **2001**, *37*, 183–188. [[CrossRef](#)]

32. Claessen, G.; La Gerche, A.; Voigt, J.U.; Dymarkowski, S.; Schnell, F.; Petit, T.; Willems, R.; Claus, P.; Delcroix, M.; Heidebuchel, H. Accuracy of Echocardiography to Evaluate Pulmonary Vascular and RV Function during Exercise. *JACC Cardiovasc. Imaging* **2016**, *9*, 532–543. [[CrossRef](#)]
33. Ghio, S.; Guazzi, M.; Scardovi, A.B.; Klersy, C.; Clemenza, F.; Carluccio, E.; Temporelli, P.L.; Rossi, A.; Faggiano, P.; Traversi, E.; et al. Different correlates but similar prognostic implications for right ventricular dysfunction in heart failure patients with reduced or preserved ejection fraction. *Eur. J. Heart Fail.* **2017**, *19*, 873–879. [[CrossRef](#)]
34. Vriz, O.; Pirisi, M.; Bossoni, E.; Fadl Elmula, F.E.M.; Palatini, P.; Naeije, R. Right ventricular-pulmonary arterial uncoupling in mild-to-moderate systemic hypertension. *J. Hypertens.* **2020**, *38*, 274–281. [[CrossRef](#)]
35. Nie, L.; Li, J.; Zhang, S.; Dong, Y.; Xu, M.; Yan, M.; Zhang, G.; Song, L. Correlation between right ventricular-pulmonary artery coupling and the prognosis of patients with pulmonary arterial hypertension. *Medicine* **2019**, *98*, e5353. [[CrossRef](#)]
36. Huston, J.H.; Maron, B.A.; French, J.; Huang, S.; Thayer, T.; Farber-Eger, E.H.; Wells, Q.S.; Choudhary, G.; Hemnes, A.R.; Brittain, E.L. Association of Mild Echocardiographic Pulmonary Hypertension with Mortality and Right Ventricular Function. *JAMA Cardiol.* **2019**, *4*, 1112–1121. [[CrossRef](#)]
37. Li, Y.; Guo, D.; Gong, J.; Wang, J.; Huang, Q.; Yang, S.; Zhang, X.; Hu, H.; Jiang, Z.; Yang, Y.; et al. Right Ventricular Function and Its Coupling with Pulmonary Circulation in Precapillary Pulmonary Hypertension: A Three-Dimensional Echocardiographic Study. *Front. Cardiovasc. Med.* **2021**, *8*, 690606. [[CrossRef](#)]
38. Jentzer, J.C.; Anavekar, N.S.; Reddy, Y.N.V.; Murphree, D.H.; Wiley, B.M.; Oh, J.K.; Borlaug, B.A. Right ventricular pulmonary artery coupling and mortality in cardiac intensive care unit patients. *J. Am. Heart Assoc.* **2021**, *10*, e019015. [[CrossRef](#)]
39. Gao, H.Y.; Wang, X.J.; Deng, A.Y. Progress in echocardiographic evaluation of right ventricular function in patients with pulmonary hypertension. *Med. Recapitul.* **2018**, *24*, 1409–1413.
40. Egbe, A.C.; Kothapalli, S.; Miranda, W.R.; Pislaru, S.; Ammash, N.M.; Borlaug, B.A.; Pellikka, P.A.; Najam, M.; Connolly, H.M. Assessment of Right Ventricular-Pulmonary Arterial Coupling in Chronic Pulmonary Regurgitation. *Can. J. Cardiol.* **2019**, *35*, 914–922. [[CrossRef](#)]
41. Song, T.; Gao, X.J.; Zhao, L. The value of right atrial area and two-dimensional right ventricular area change score in the evaluation of right ventricular function. *Chin. J. Mod. Drug Appl.* **2016**, *10*, 51–52. [[CrossRef](#)]
42. Sanz, J.; García-Alvarez, A.; Fernández-Friera, L.; Nair, A.; Mirelis, J.G.; Sawit, S.T.; Pinney, S.; Fuster, V. Right ventriculo-arterial coupling in pulmonary hypertension: A magnetic resonance study. *Heart* **2012**, *98*, 238–243. [[CrossRef](#)]
43. Brewis, M.J.; Bellofiore, A.; Vanderpool, R.R.; Chesler, N.C.; Johnson, M.K.; Naeije, R.; Peacock, A.J. Imaging right ventricular function to predict outcome in pulmonary arterial hypertension. *Int. J. Cardiol.* **2016**, *218*, 206–211. [[CrossRef](#)]
44. Truong, U.; Patel, S.; Kheyfets, V.; Dunning, J.; Fonseca, B.; Barker, A.J.; Ivy, D.; Shandas, R.; Hunter, K. Non-invasive determination by cardiovascular magnetic resonance of right ventricular-vascular coupling in children and adolescents with pulmonary hypertension. *J. Cardiovasc. Magn. Reson.* **2015**, *17*, 81. [[CrossRef](#)]
45. Vîjtiac, A.; Onciul, S.; Deaconu, S.; Vătăşescu, R.; Guzu, C.; Verinceanu, V.; Scărlătescu, A.; Zamfir, D.; Petre, I.; Scafa-Udrişte, A.; et al. Three-dimensional right ventriculo-arterial coupling as an independent determinant of severe heart failure symptoms in patients with dilated cardiomyopathy. *Echocardiography* **2022**, *39*, 194–203. [[CrossRef](#)]
46. Aubert, R.; Venner, C.; Huttin, O.; Haine, D.; Filippetti, L.; Guillaumot, A.; Mandry, D.; Marie, P.Y.; Juilliere, Y.; Chabot, F.; et al. Three-Dimensional Echocardiography for the Assessment of Right Ventriculo-Arterial Coupling. *J. Am. Soc. Echocardiogr.* **2018**, *31*, 905–915. [[CrossRef](#)]
47. Jone, P.N.; Schäfer, M.; Pan, Z.; Ivy, D.D. Right Ventricular-Arterial Coupling Ratio Derived From 3-Dimensional Echocardiography Predicts Outcomes in Pediatric Pulmonary Hypertension. *Circ. Cardiovasc. Imaging* **2019**, *12*, e008176. [[CrossRef](#)]
48. Trip, P.; Kind, T.; Van De Veerdonk, M.C.; Marcus, J.T.; De Man, F.S.; Westerhof, N.; Vonk-Noordegraaf, A. Accurate assessment of load-independent right ventricular systolic function in patients with pulmonary hypertension. *J. Heart Lung Transplant.* **2013**, *32*, 50–55. [[CrossRef](#)]
49. Iacoviello, M.; Citarelli, G.; Antoncicchi, V.; Romito, R.; Monitillo, F.; Leone, M.; Puzzovivo, A.; Lattarulo, M.S.; Rizzo, C.; Caldarola, P.; et al. Right Ventricular Longitudinal Strain Measures Independently Predict Chronic Heart Failure Mortality. *Echocardiography* **2016**, *33*, 992–1000. [[CrossRef](#)]
50. Brener, M.I.; Grayburn, P.; Lindenfeld, J.A.; Burkhoff, D.; Liu, M.; Zhou, Z.; Alu, M.C.; Medvedofsky, D.A.; Asch, F.M.; Weissman, N.J.; et al. Right Ventricular–Pulmonary Arterial Coupling in Patients with HF Secondary MR: Analysis from the COAPT Trial. *JACC Cardiovasc. Interv.* **2021**, *14*, 2231–2242. [[CrossRef](#)]
51. Richter, M.J.; Rako, Z.A.; Tello, K. Ratio between right ventricular strain and systolic pulmonary artery pressure as a surrogate for right ventricular to pulmonary arterial coupling: Validation against the gold standard. *Eur. Heart J. -Cardiovasc. Imaging* **2022**, *24*, e50–e52. [[CrossRef](#)]
52. Ünlü, S.; Bézy, S.; Cvijic, M.; Duchenne, J.; Delcroix, M.; Voigt, J.U. Right ventricular strain related to pulmonary artery pressure predicts clinical outcome in patients with pulmonary arterial hypertension. *Eur. Heart J. Cardiovasc. Imaging* **2022**, jeac136. [[CrossRef](#)]
53. Nagata, Y.; Wu, V.C.C.; Kado, Y.; Otani, K.; Lin, F.C.; Otsuji, Y.; Negishi, K.; Takeuchi, M. Prognostic Value of Right Ventricular Ejection Fraction Assessed by Transthoracic 3D Echocardiography. *Circ. Cardiovasc. Imaging* **2017**, *10*, e005384. [[CrossRef](#)]

54. Van De Veerdonk, M.C.; Kind, T.; Marcus, J.T.; Mauritz, G.J.; Heymans, M.W.; Bogaard, H.J.; Boonstra, A.; Marques, K.M.; Westerhof, N.; Vonk-Noordegraaf, A. Progressive right ventricular dysfunction in patients with pulmonary arterial hypertension responding to therapy. *J. Am. Coll. Cardiol.* **2011**, *58*, 2511–2519. [[CrossRef](#)]
55. Jimenez-Juan, L.; Ben-Dov, N.; Goncalves Frazao, C.V.; Tan, N.S.; Singh, S.M.; Dorian, P.; Angaran, P.; Oikonomou, A.; Kha, L.T.; Roifman, I.; et al. Right ventricular function at cardiac MRI predicts cardiovascular events in patients with an implantable cardioverter-defibrillator. *Radiology* **2021**, *301*, 322–329. [[CrossRef](#)]
56. Nochioka, K.; Querejeta Roca, G.; Claggett, B.; Biering-Sørensen, T.; Matsushita, K.; Hung, C.L.; Solomon, S.D.; Kitman, D.; Shah, A.M. Right Ventricular Function, Right Ventricular–Pulmonary Artery Coupling, and Heart Failure Risk in 4 US Communities: The Atherosclerosis Risk in Communities (ARIC) Study. *JAMA Cardiol.* **2018**, *3*, 939–948. [[CrossRef](#)]
57. Hoepfer, M.M.; Huscher, D.; Ghofrani, H.A.; Delcroix, M.; Distler, O.; Schweiger, C.; Grunig, E.; Staehler, G.; Rosenkranz, S.; Halank, M.; et al. Elderly patients diagnosed with idiopathic pulmonary arterial hypertension: Results from the COMPERA registry. *Int. J. Cardiol.* **2013**, *168*, 871–880. [[CrossRef](#)]
58. Bossone, E.; D’Andrea, A.; D’Alto, M.; Citro, R.; Argiento, P.; Ferrara, F.; Cittadini, A.; Rubenfire, M.; Naeije, R. Echocardiography in pulmonary arterial hypertension: From diagnosis to prognosis. *J. Am. Soc. Echocardiogr.* **2013**, *26*, 1–14. [[CrossRef](#)]
59. Vonk Noordegraaf, A.; Westerhof, B.E.; Westerhof, N. The Relationship Between the Right Ventricle and its Load in Pulmonary Hypertension. *J. Am. Coll. Cardiol.* **2017**, *69*, 236–243. [[CrossRef](#)]
60. Vonk Noordegraaf, A.; Haddad, F.; Bogaard, H.J.; Hassoun, P.M. Noninvasive imaging in the assessment of the cardiopulmonary vascular unit. *Circulation* **2015**, *131*, 899–913. [[CrossRef](#)]
61. Leurent, G.; Auffret, V.; Donal, E. Right Ventricular–Pulmonary Artery Coupling: A Simple Marker to Guide Complex Clinical Decisions? *JACC Cardiovasc. Interv.* **2022**, *15*, 1834–1836. [[CrossRef](#)]
62. Yang, Y.H. Interpretation of Chinese guidelines for diagnosis and treatment of Pulmonary Hypertension (2021 Edition)- diagnosis of Pulmonary Hypertension. *Chin. J. Pr. Intern. Med.* **2021**, *41*, 696–699. [[CrossRef](#)]
63. Bellettini, M.; Frea, S.; Pidello, S.; Boffini, M.; Boretto, P.; Gallone, G.; Bongiovanni, F.; Masetti, M.; Sabatino, M.; Raineri, C.; et al. Pretransplant Right Ventricular Dysfunction Is Associated with Increased Mortality After Heart Transplantation: A Hard Inheritance to Overcome. *J. Card Fail.* **2022**, *28*, 259–269. [[CrossRef](#)]
64. Nazario, R.A.; Goldraich, L.A.; Hastenteufel, L.C.T.; Santos, A.B.S.; Carrion, L.; Clausell, N. Donor-recipient predicted heart mass ratio and right ventricular-pulmonary arterial coupling in heart transplant. *Eur. J. Cardiothorac. Surg.* **2021**, *59*, 847–854. [[CrossRef](#)] [[PubMed](#)]
65. López-Candales, A.; Lopez, F.R.; Trivedi, S.; Elwing, J. Right ventricular ejection efficiency: A new echocardiographic measure of mechanical performance in chronic pulmonary hypertension. *Echocardiography* **2014**, *31*, 516–523. [[CrossRef](#)]
66. Ponikowski, P.; Voors, A.A.; Anker, S.D.; Bueno, H.; Cleland, J.G.; Coats, A.J.; Falk, V.; González-Juanatey, J.R.; Harjola, V.P.; Jankowska, E.A.; et al. 2016 ESC Guidelines for the diagnosis and treatment of acute and chronic heart failure. *Eur. Heart J.* **2016**, *37*, 2129–2200. [[CrossRef](#)]
67. Bauersachs, J.; Bozkurt, B.; Boer, R.A.D.; Lindenfeld, J. The year in cardiovascular medicine 2021: Heart failure and cardiomyopathies. *Cardiol. Croat.* **2022**, *17*, 367–376. [[CrossRef](#)]
68. Withaar, C.; Lam, C.S.P.; Schiattarella, G.G.; De Boer, R.A.; Meems, L.M.G. Heart failure with preserved ejection fraction in humans and mice: Embracing clinical complexity in mouse models. *Eur. Heart J.* **2021**, *42*, 4420–4430. [[CrossRef](#)]
69. Jering, K.; Claggett, B.; Redfield, M.M.; Shah, S.J.; Anand, I.S.; Martinez, F.; Sabarwal, S.V.; Seferović, P.M.; Kerr Saraiva, J.F.; Katova, T.; et al. Burden of Heart Failure Signs and Symptoms, Prognosis, and Response to Therapy: The PARAGON-HF Trial. *JACC Heart Fail.* **2021**, *9*, 386–397. [[CrossRef](#)]
70. Bozkurt, B.; Coats, A.J.S.; Tsutsui, H.; Abdelhamid, C.M.; Adamopoulos, S.; Albert, N.; Anker, S.D.; Atherton, J.; Böhm, M.; Butler, J.; et al. Universal definition and classification of heart failure: A report of the Heart Failure Society of America, Heart Failure Association of the European Society of Cardiology, Japanese Heart Failure Society and Writing Committee of the Universal Definition of Heart Failure. *Eur. J. Heart Fail.* **2021**, *23*, 352–380. [[CrossRef](#)]
71. Yancy, C.W.; Jessup, M.; Bozkurt, B.; Butler, J.; Casey, D.E.; Colvin, M.M.; Drazner, M.H.; Filippatos, G.S.; Fonarow, G.C.; Givertz, M.M.; et al. 2017 ACC/AHA/HFSA Focused Update of the 2013 ACCF/AHA Guideline for the Management of Heart Failure: A Report of the American College of Cardiology/American Heart Association Task Force on Clinical Practice Guidelines and the Heart Failure Society of America. *Circulation* **2017**, *136*, e137–e161. [[CrossRef](#)] [[PubMed](#)]
72. Savarese, G.; Stolfo, D.; Sinagra, G.; Lund, L.H. Heart failure with mid-range or mildly reduced ejection fraction. *Nat. Rev. Cardiol.* **2022**, *19*, 100–116. [[CrossRef](#)]
73. Ghio, S.; Temporelli, P.L.; Klersy, C.; Simioniu, A.; Girardi, B.; Scelsi, L.; Rossi, A.; Ciccoira, M.; Genta, F.T.; Dini, F.L. Prognostic relevance of a non-invasive evaluation of right ventricular function and pulmonary artery pressure in patients with chronic heart failure. *Eur. J. Heart Fail.* **2013**, *15*, 408–414. [[CrossRef](#)] [[PubMed](#)]
74. Singh, I.; Oliveira, R.K.F.; Heerd, P.M.; Pari, R.; Systrom, D.M.; Waxman, A.B. Sex-Related Differences in Dynamic Right Ventricular–Pulmonary Vascular Coupling in Heart Failure with Preserved Ejection Fraction. *Chest* **2021**, *159*, 2402–2416. [[CrossRef](#)]
75. Owan, T.E.; Hodge, D.O.; Herges, R.M.; Jacobsen, S.J.; Roger, V.L.; Redfield, M.M. Trends in Prevalence and Outcome of Heart Failure with Preserved Ejection Fraction. *N. Engl. J. Med.* **2006**, *355*, 251–259. [[CrossRef](#)]
76. Maeder, M.T.; Thompson, B.R.; Brunner-La Rocca, H.P.; Kaye, D.M. Hemodynamic basis of exercise limitation in patients with heart failure and normal ejection fraction. *J. Am. Coll. Cardiol.* **2010**, *56*, 855–863. [[CrossRef](#)]

77. Borlaug, B.A.; Nishimura, R.A.; Sorajja, P.; Lam, C.S.P.; Redfield, M.M. Exercise hemodynamics enhance diagnosis of early heart failure with preserved ejection fraction. *Circ. Heart Fail.* **2010**, *3*, 588–595. [[CrossRef](#)]
78. Abudiab, M.M.; Redfield, M.M.; Melenovsky, V.; Olson, T.P.; Kass, D.A.; Johnson, B.D.; Borlaug, B.A. Cardiac output response to exercise in relation to metabolic demand in heart failure with preserved ejection fraction. *Eur. J. Heart Fail.* **2013**, *15*, 776–785. [[CrossRef](#)]
79. Ennezat, P.V.; Lefetz, Y.; Maréchaux, S.; Six-Carpentier, M.; Deklunder, G.; Montaigne, D.; Bauchart, J.J.; Mounier-Véhier, C.; Jude, B.; Nevière, R.; et al. Left Ventricular Abnormal Response During Dynamic Exercise in Patients with Heart Failure and Preserved Left Ventricular Ejection Fraction at Rest. *J. Card. Fail.* **2008**, *14*, 475–480. [[CrossRef](#)]
80. Tan, Y.T.; Wenzelburger, F.; Lee, E.; Heatlie, G.; Leyva, F.; Patel, K.; Frenneaux, M.; Sanderson, J.E. The Pathophysiology of Heart Failure with Normal Ejection Fraction. Exercise Echocardiography Reveals Complex Abnormalities of Both Systolic and Diastolic Ventricular Function Involving Torsion, Untwist, and Longitudinal Motion. *J. Am. Coll. Cardiol.* **2009**, *54*, 36–46. [[CrossRef](#)]
81. Phan, T.T.; Abozguia, K.; Nallur Shivu, G.; Mahadevan, G.; Ahmed, I.; Williams, L.; Dwivedi, G.; Patel, K.; Steendijk, P.; Ashrafian, H.; et al. Heart Failure with Preserved Ejection Fraction Is Characterized by Dynamic Impairment of Active Relaxation and Contraction of the Left Ventricle on Exercise and Associated with Myocardial Energy Deficiency. *J. Am. Coll. Cardiol.* **2009**, *54*, 402–409. [[CrossRef](#)] [[PubMed](#)]
82. Borlaug, B.A.; Olson, T.P.; Lam, C.S.P.; Flood, K.S.; Lerman, A.; Johnson, B.D.; Redfield, M.M. Global cardiovascular reserve dysfunction in heart failure with preserved ejection fraction. *J. Am. Coll. Cardiol.* **2010**, *56*, 845–854. [[CrossRef](#)] [[PubMed](#)]
83. Lam, C.S.P.; Roger, V.L.; Rodeheffer, R.J.; Borlaug, B.A.; Enders, F.T.; Redfield, M.M. Pulmonary Hypertension in Heart Failure with Preserved Ejection Fraction. A Community-Based Study. *J. Am. Coll. Cardiol.* **2009**, *53*, 1119–1126. [[CrossRef](#)] [[PubMed](#)]
84. Mohammed, S.F.; Hussain, I.; Abou Ezzeddine, O.F.; Takahama, H.; Kwon, S.H.; Forfia, P.; Roger, V.L.; Redfield, M.M. Right ventricular function in heart failure with preserved ejection fraction: A community-based study. *Circulation* **2014**, *130*, 2310–2320. [[CrossRef](#)]
85. Burke, M.A.; Katz, D.A.; Beussink, L.; Selvaraj, S.; Gupta, D.K.; Fox, J.; Chakrabarti, S.; Sauer, A.J.; Rich, J.D.; Freed, B.H.; et al. Prognostic importance of pathophysiologic markers in patients with heart failure and preserved ejection fraction. *Circ. Heart Fail.* **2014**, *7*, 288–299. [[CrossRef](#)]
86. Reddy, Y.N.V.; Obokata, M.; Koepp, K.E.; Egbe, A.C.; Wiley, B.; Borlaug, B.A. The β -Adrenergic Agonist Albuterol Improves Pulmonary Vascular Reserve in Heart Failure with Preserved Ejection Fraction: A Randomized Controlled Trial. *Circ. Res.* **2019**, *124*, 306–314. [[CrossRef](#)]
87. Berglund, F.; Piña, P.; Herrera, C.J. Right ventricle in heart failure with preserved ejection fraction. *Heart* **2020**, *106*, 1798–1804. [[CrossRef](#)]
88. Singh, I.; Oliveira, R.K.F.; Naeije, R.; Rahaghi, F.N.; Oldham, W.M.; Systrom, D.M.; Waxman, A.B. Pulmonary Vascular Distensibility and Early Pulmonary Vascular Remodeling in Pulmonary Hypertension. *Chest* **2019**, *156*, 724–732. [[CrossRef](#)]
89. Singh, I.; Rahaghi, F.N.; Naeije, R.; Oliveira, R.K.F.; Systrom, D.M.; Waxman, A.B. Right Ventricular-Arterial Uncoupling During Exercise in Heart Failure with Preserved Ejection Fraction: Role of Pulmonary Vascular Dysfunction. *Chest* **2019**, *156*, 933–943. [[CrossRef](#)]
90. Andersen, M.J.; Hwang, S.J.; Kane, G.C.; Melenovsky, V.; Olson, T.P.; Fetterly, K.; Borlaug, B.A. Enhanced Pulmonary Vasodilator Reserve and Abnormal Right Ventricular: Pulmonary Artery Coupling in Heart Failure with Preserved Ejection Fraction. *Circ. Heart Fail.* **2015**, *8*, 542–550. [[CrossRef](#)]
91. Reddy, Y.N.V.; Obokata, M.; Wiley, B.; Koepp, K.E.; Jorgenson, C.C.; Egbe, A.; Melenovsky, V.; Carter, R.E.; Borlaug, B.A. The haemodynamic basis of lung congestion during exercise in heart failure with preserved ejection fraction. *Eur. Heart J.* **2019**, *40*, 3721–3730. [[CrossRef](#)] [[PubMed](#)]
92. Schmeißer, A.; Rauwolf, T.; Groscheck, T.; Fischbach, K.; Kropf, S.; Luani, B.; Tanev, I.; Hansen, M.; Meißler, S.; Schäfer, K.; et al. Predictors and prognosis of right ventricular function in pulmonary hypertension due to heart failure with reduced ejection fraction. *ESC Heart Fail.* **2021**, *8*, 2968–2981. [[CrossRef](#)] [[PubMed](#)]
93. Legris, V.; Thibault, B.; Dupuis, J.; White, M.; Asgar, A.W.; Fortier, A.; Pitre, C.; Bouabdallaoui, N.; Henri, C.; O’Meara, E.; et al. Right ventricular function and its coupling to pulmonary circulation predicts exercise tolerance in systolic heart failure. *ESC Heart Fail.* **2022**, *9*, 450–464. [[CrossRef](#)]
94. Deaconu, S.; Deaconu, A.; Scarlatescu, A.; Petre, I.; Onciul, S.; Vijiac, A.; Onut, R.; Zamfir, D.; Marascu, G.; Iorgulescu, C.; et al. Right ventricular-arterial coupling—A new perspective for right ventricle evaluation in heart failure patients undergoing cardiac resynchronization therapy. *Echocardiography* **2021**, *38*, 1157–1164. [[CrossRef](#)]
95. Hu, M.; Kang, Y.; Jiang, J. Evaluation of right atrial structure and function in patients with chronic Heart failure and Hypertension by Echocardiography. *Imaging Res. Med. Appl.* **2021**, *5*, 54–55.
96. Tadic, M.; Cuspidi, C.; Suzic-Lazic, J.; Andric, A.; Stojcevski, B.; Ivanovic, B.; Hot, S.; Scepanovic, R.; Celic, V. Is there a relationship between right-ventricular and right atrial mechanics and functional capacity in hypertensive patients? *J. Hypertens.* **2014**, *32*, 929–937. [[CrossRef](#)]
97. Sciacqua, A.; Perticone, M.; Miceli, S.; Pinto, A.; Cassano, V.; Succurro, E.; Andreozzi, F.; Hribal, M.L.; Sesti, G.; Perticone, F. Elevated 1-h post-load plasma glucose is associated with right ventricular morphofunctional parameters in hypertensive patients. *Endocrine* **2019**, *64*, 525–535. [[CrossRef](#)]

98. Sun, H.; Chen, C.H.; Bao, L. Evaluation of right Atrial structure and function in patients with Hypertension and chronic Heart failure by Echocardiography. *Chin. J. Geriatr. Cardiovasc. Cerebrovasc. Dis.* **2019**, *21*, 1171–1173.
99. Fortuni, F.; Butcher, S.C.; Dietz, M.F.; Van der Bijl, P.; Prihadi, E.A.; De Ferrari, G.M.; Ajmone Marsan, N.; Bax, J.J.; Delgado, V. Right Ventricular–Pulmonary Arterial Coupling in Secondary Tricuspid Regurgitation. *Am. J. Cardiol.* **2021**, *148*, 138–145. [[CrossRef](#)]
100. Azpiri-Lopez, J.R.; Galarza-Delgado, D.A.; Colunga-Pedraza, I.J.; Arvizu-Rivera, R.I.; Cardenas-de la Garza, J.A.; Vera-Pineda, R.; Davila-Jimenez, J.A.; Martinez-Flores, C.M.; Rodriguez-Romero, A.B.; Guajardo-Jauregui, N. Echocardiographic evaluation of pulmonary hypertension, right ventricular function, and right ventricular-pulmonary arterial coupling in patients with rheumatoid arthritis. *Clin. Rheumatol.* **2021**, *40*, 2651–2656. [[CrossRef](#)]
101. Eleid, M.F.; Padang, R.; Pislaru, S.V.; Greason, K.L.; Crestanello, J.; Nkomo, V.T.; Pellikka, P.A.; Jentzer, J.C.; Gulati, R.; Sandhu, G.S. Effect of Transcatheter Aortic Valve Replacement on Right Ventricular–Pulmonary Artery Coupling. *JACC Cardiovasc. Interv.* **2019**, *12*, 2145–2154. [[CrossRef](#)] [[PubMed](#)]
102. Egbe, A.C.; Miranda, W.R.; Pellikka, P.A.; Pislaru, S.V.; Borlaug, B.A.; Kothapalli, S.; Ananthaneni, S.; Sandhyavenu, H.; Najam, M.; Farouk Abdelsamid, M. Right ventricular and pulmonary vascular function indices for risk stratification of patients with pulmonary regurgitation. *Congenit. Heart Dis.* **2019**, *14*, 657–664. [[CrossRef](#)] [[PubMed](#)]
103. Pinto, Y.M.; Elliott, P.M.; Arbustini, E.; Adler, Y.; Anastasakis, A.; Böhm, M.; Duboc, D.; Gimeno, J.; de Groote, P.; Imazio, M. Proposal for a revised definition of dilated cardiomyopathy, hypokinetic non-dilated cardiomyopathy, and its implications for clinical practice: A position statement of the ESC working group on myocardial and pericardial diseases. *Eur. Heart J.* **2016**, *37*, 1850–1858. [[CrossRef](#)] [[PubMed](#)]
104. Merlo, M.; Cannatà, A.; Gobbo, M.; Stolfo, D.; Elliott, P.M.; Sinagra, G. Evolving concepts in dilated cardiomyopathy. *Eur. J. Heart Fail.* **2018**, *20*, 228–239. [[CrossRef](#)] [[PubMed](#)]
105. Vîjtiac, A.; Bătăiță, V.; Onciul, S.; Verinceanu, V.; Guzu, C.; Deaconu, S.; Petre, I.; Scărlătescu, A.; Zamfir, D.; Dorobanțu, M. Non-invasive right ventriculo-arterial coupling as a rehospitalization predictor in dilated cardiomyopathy: A comparison of five different methods. *Kardiol. Pol.* **2022**, *80*, 182–190. [[CrossRef](#)]
106. Hirasawa, K.; Izumo, M.; Mizukoshi, K.; Nishikawa, H.; Sato, Y.; Watanabe, M.; Kamijima, R.; Akashi, Y.J. Prognostic significance of right ventricular function during exercise in asymptomatic/minimally symptomatic patients with nonobstructive hypertrophic cardiomyopathy. *Echocardiography* **2021**, *38*, 916–923. [[CrossRef](#)]

Disclaimer/Publisher’s Note: The statements, opinions and data contained in all publications are solely those of the individual author(s) and contributor(s) and not of MDPI and/or the editor(s). MDPI and/or the editor(s) disclaim responsibility for any injury to people or property resulting from any ideas, methods, instructions or products referred to in the content.